

GBES antenna Efficiency Measurements of April 1994

Glen Langston

95 January 24

Overview

This document describes measurements and calculations of the OVLBI GBES antenna gain in April 1994 when observing at 14.35 GHz. The antenna efficiency was measured by observations of radio sources of known brightness and small angular size. The antenna efficiency has not changed significantly since 1991, although a possible decrease in efficiency is noted. The addition of the FSS and ellipsoid appear to detract little from the total antenna efficiency. Data are presented which show the radome is transparent in the Ku band. Appendix A describes the observing technique used to measure the radio source brightness.

Introduction

The absolute of efficiency of antennas can be measured by observation of bright radio sources (e.g. Baars, J. W. M. (1973), *IEEE Transactions on Antennas and Propagation* AP-21, No 4:461). In order to measure the efficiency of the GBES 45', bright radio source Cassiopeia A was observed continuously for 20 hours on 94 April 25. Radio source Cygnus A was observed for 4 hours on 94 April 26. A plot of the azimuth and elevation of these sources during the observations is shown in figure 1. During these days the weather was partly cloudy and, by coincidence, when the sources were at approximately 0.6 radians elevation, rain showers adversely effected source measurements, due to sky brightness variations.

Short observations of Tau A, Vir A, Ori A, 3C84 and 3C273 were made on 94 April 27. These observations were made with the ellipsoidal mirror and frequency selective surface (FSS) in place (see GBES Memo 18 by B. Shillue). The subreflector focus voltage was 1.32 V and the subreflector rotation voltage was 4.95 V. These observations were made with the Right Circularly Polarized channel of the Ku band feed over the band 14.1 to 14.6 GHz. The antenna gain was calibrated assuming an injected calibration noise diode temperature of 4.2 ± 0.3 K.

These measurements were made without the radome, but with 4 thin sheets of clear plastic taped over the FSS and ellipsoid. On one good weather day, observations were made without the plastic sheets. The observations showed the plastic is nearly completely transparent at 2cm (absorption less than 1 %). One of the inner panels of the antenna was removed to allow access to the optics. There are 24 inner panels on the antenna and 48 outer panels. Removing one inner panel is believed to reduce the antenna efficiency by less than 1 %.

In memo GBES memo 14, by L. D'Addario, the antenna temperature is calculated for these radio sources for 100 % antenna efficiency. The predicted values are listed in table 1, with

Source Name	Flux Density at 14.9 GHz (Jy)	Angular Size (arcmin)	Resolution Factor Assumed	Antenna T Ideal (K)	Antenna T Measured (K)	Aperture Efficiency
Cas A	317.3	3	0.800	16.99	5.25±.05	0.39±.01
Cyg A	93.3	1×2	0.950	5.00	1.70±.10	0.36±.02
Tau A	464.7	3×5	0.706	24.90	7.71±.10	0.44±.01
Vir A	27.5	<1	1.000	1.47	0.57±.02	0.39±.01
3C84	Variable	<1	1.000		0.73±.10	
3C273	Variable	<1	1.000		0.66±.10	
at 14.35 GHz						
	(Jy)					
Cas A	354.8		0.800	19.00	5.20±.10	0.34±.02
Cyg A	104.8		0.950	5.62	1.68±.05	0.31±.02
Tau A	488.3		0.706	26.16	7.08±.05	0.38±.01
Vir A	29.4		1.000	1.58	0.58±.05	0.37±.03
3C84					0.53±.05	
3C273					0.78±.02	
Ori A					0.44±.02	

Table 1: Measurements of the antenna efficiency in 1991 (top) and 1994 April (bottom). The flux densities are based on values reported in Baars (1973).

measurements of the antenna efficiency in 1991. The 1991 observations were made with a prime focus beam switching receiver operating at a center frequency of 14.9 GHz. In the bottom section of table 1, the 94 April 23-27 measurements are listed.

The 1994 measurements of efficiency can not be directly compared to the 1991 measurements since the observing frequency and bandwidth were different (the receiver and feeds were completely different). The 1991 measurements were made with a prime focus receiver. Also the radio sources are known to be time variable at the few percent level. The antenna efficiency was expected to be greater at 14.35 GHz than at 14.9 GHz.

Antenna Gain versus Elevation

The source brightness as a function of elevation was determined by the 1994 measurements. Figure 2. shows the intensity of Cas A and Cygnus A as a function of antenna elevation. The peak intensity of Cas A drops by 19 % as the antenna elevation changes from 90 to 20 degrees. The large random variations in source brightness are believed to be due to incorrect subtraction of the sky background during periods of bad weather. Appendix A contains a more detailed description of the source measurement process.

Figure 3. shows the measured source size of Cas A as a function of antenna elevation. Notice the increase in measured size with decreasing elevation. At 90 degrees elevation, the measured size is 7.5 arc minutes and at 20 degrees elevation, the measured size is 7.75 arc

minutes. The source peak intensity is decreased by a factor of $(7.5/7.75)^2 \sim 0.93$, a 7 % decrease due to the increased beam size. The large scatter in points near elevation 0.6 are due to bad weather during these observations.

Below 15 degrees elevation, the Cas A data are not reliable, because the control trailer shadows antenna when the antenna is pointed due north.

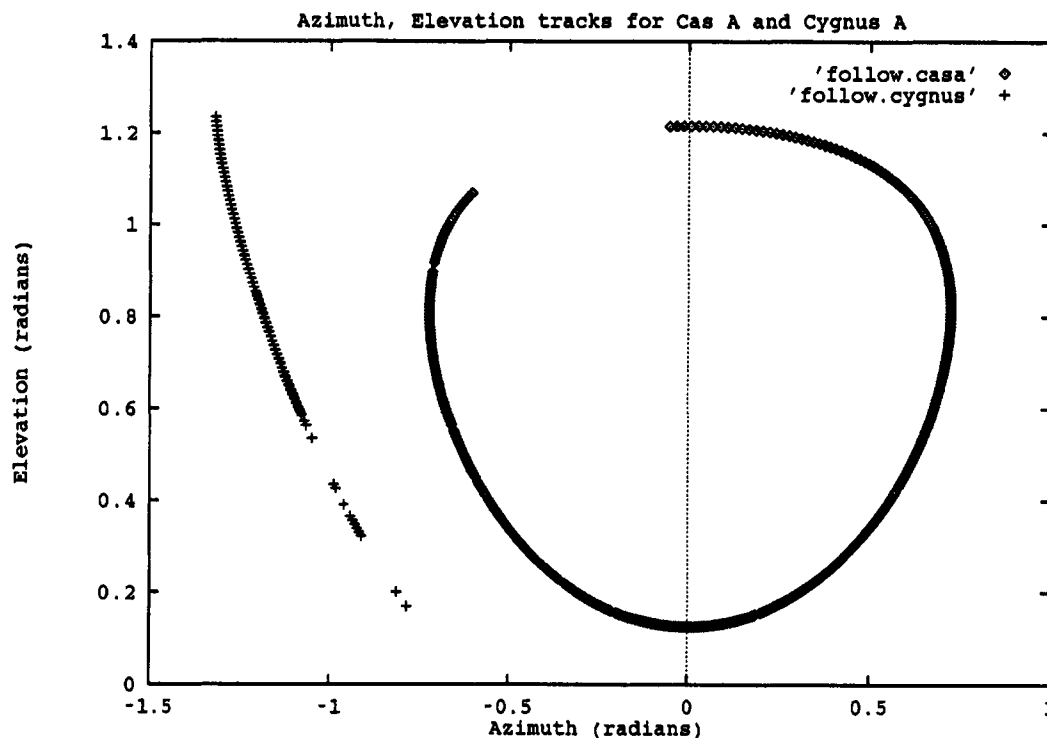


Figure 1: Plot of the Azimuth and Elevation (radians) locations of the radio sources when gain measurements were taken.

Radome

On 94 April 28, the radome was installed and on 94 April 29, pointing data were again taken. Figure 4 shows observations of Cas A show antenna temperature is unchanged with the radome, indicating the radome is highly transparent.

Tipping Curves

Figure 5 shows two scans of the sky from 84 to 4 degrees elevation at azimuth -135 degrees. The data have an arbitrary offset in the Y axis, as the total system plus sky temperature was approximately 50 degrees K. The curve shows the dramatic increase in system temperature as the antenna reaches low elevations. These data were taken during the day under good weather conditions.

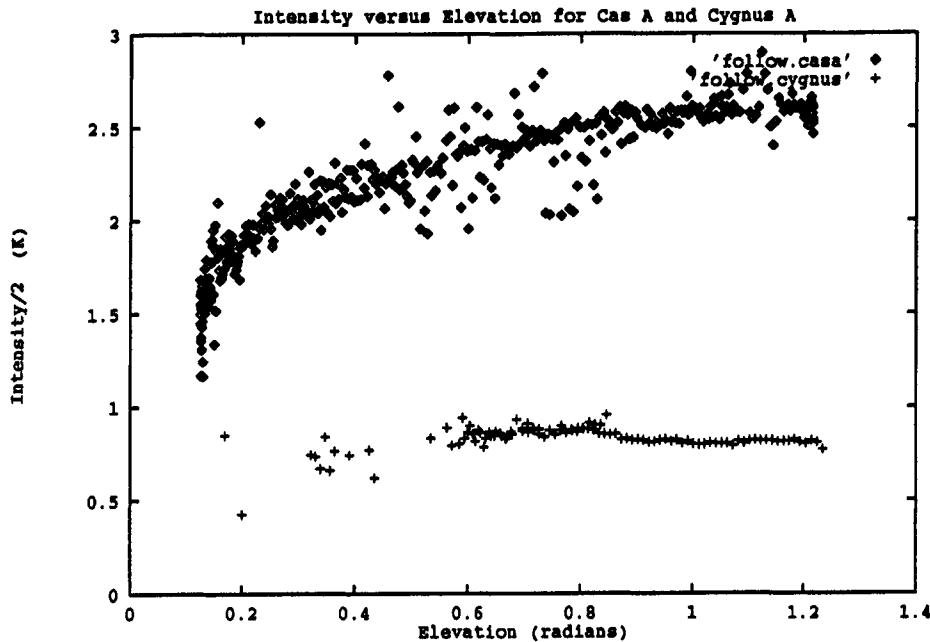


Figure 2: Plot of the half antenna temperature for the radio source as a function of source elevation when the gain measurements were taken. The + (plus) symbol indicates data for Cyg A, and the ◊ (diamond) symbol indicates data for Cas A.

Conclusions

The efficiency of the GBES 45' antenna at 14.35 GHz with the ellipsoid, FSS and radome is consistent with expectations. The either the ellipsoid and FSS nor the radome made significant reductions in the antenna efficiency.

Measurements of antenna efficiency show it to be slightly less than as measured in 1991. Differences in the data processing and the fact that one panel is missing may explain these measured differences. Since the latest data were taken while slewing the antenna over the source, the peak intensity is slightly reduced. Motion of antenna should reduce the measured antenna efficiency by no more than 1 percent. (Test measurements were made moving the antenna very slowly, but no increase in the source brightness was seen.) Re-installing the central panel will further improve antenna efficiency by ~ 1 percent.

Measurements of the antenna gain as a function of elevation show that the antenna gain at 20 degrees elevation is 80% of the antenna gain at 45 degrees.

More measurements of the antenna efficiency are needed with the panel re-installed. Measurements are needed at X band and as function of elevation.

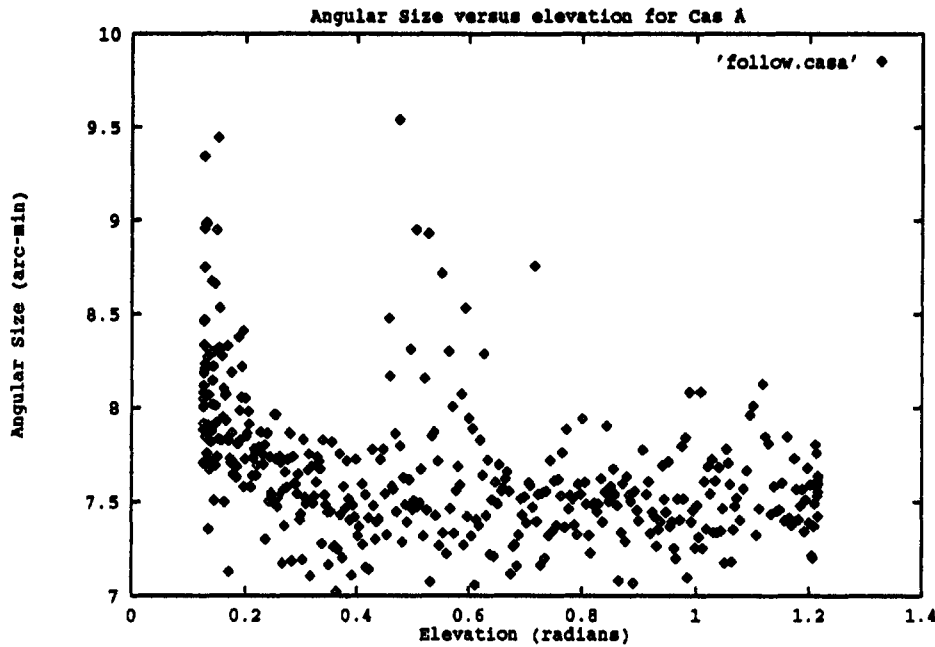


Figure 3: Plot of the Angular size of the fit to the Cas A as a function of the antenna elevation when the gain measurements were taken.

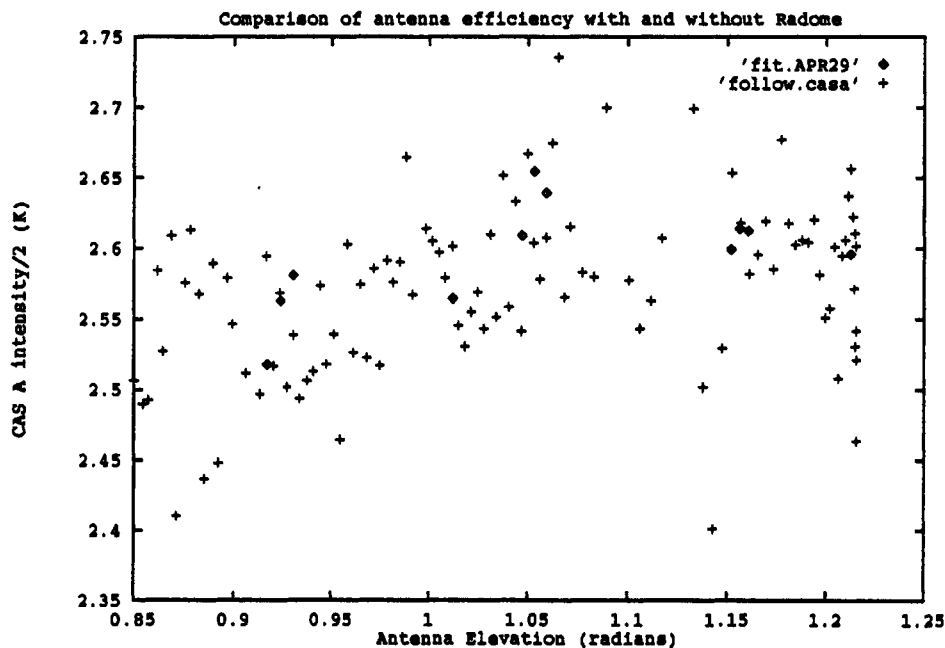


Figure 4: Plot of the Observations of the system temperature increase for the GBES at 14.1 to 14.6 GHz for radio source Cassiopeia A. The X axis is antenna elevation (radians) and the Y axis is antenna temperature. The data taken before installation of the radome are marked with a + (plus) and after installation with a ◆ (diamonds). Note there is no statistically significant difference between the average intensities, indicating the radome is transparent.

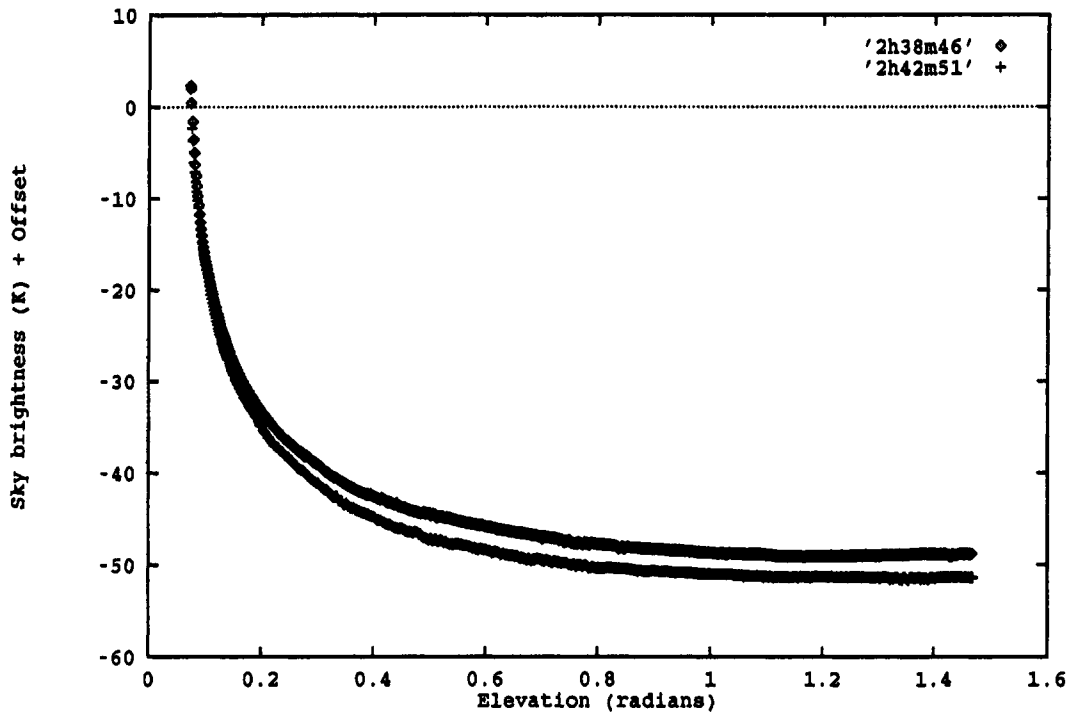


Figure 5: Plot of the sky temperature versus elevation for two scans at azimuth -135 degrees. The antenna was slewed from 84 degrees to 4 degrees elevation and back. An arbitrary offset was subtracted from the data (resulting in negative system temperatures).

Appendix A: Measurement of Source Brightness

Observation of a radio source brightness was made by scanning the antenna over the source coordinate in 4 directions, scanning each direction twice. The antenna moves 1) positive to negative azimuth, 2) negative to positive azimuth, 3) positive to negative elevation, 4) negative to positive elevation, 5) positive to negative azimuth and elevation, 6) negative to positive azimuth and elevation, 7) positive to negative azimuth and opposite in elevation, and finally 8) negative to positive azimuth and opposite in elevation. Because the antenna moves in opposite directions for all orientations, to first order, there is no position offset due to antenna motion. Figure 6 shows the pattern scanned for on measurement of brightness of Cas A. Data are taken every 0.25 seconds for 9.25 seconds in each of the 8 directions. Between each pair of motions, no data is taken for 4 seconds, to allow the antenna to arrive at the commanded position. The curved portion at the top of the elevation scan is due to allowing insufficient delay before starting the scan.

The antenna scanned the source moving at a rate of 10 degrees a minute in each of 8 directions, and data were taken at a rate of 4 times a second. The data for each of the 8 segments was median filtered to remove the sky contribution. The median window width was 30 arc-minutes so that the measurements are not sensitive to structures larger than 15 arc-minutes. After filtering, a least squares fit was made to the data, and 4 parameters were estimated. These parameters were 1) source brightness, 2) source azimuth position offset, 3) source elevation position offset, and 4) FWHM source size, assuming a circularly symmetric source.

The fitted data are recorded in tables for plotting and fitting as functions of the measurement parameters.

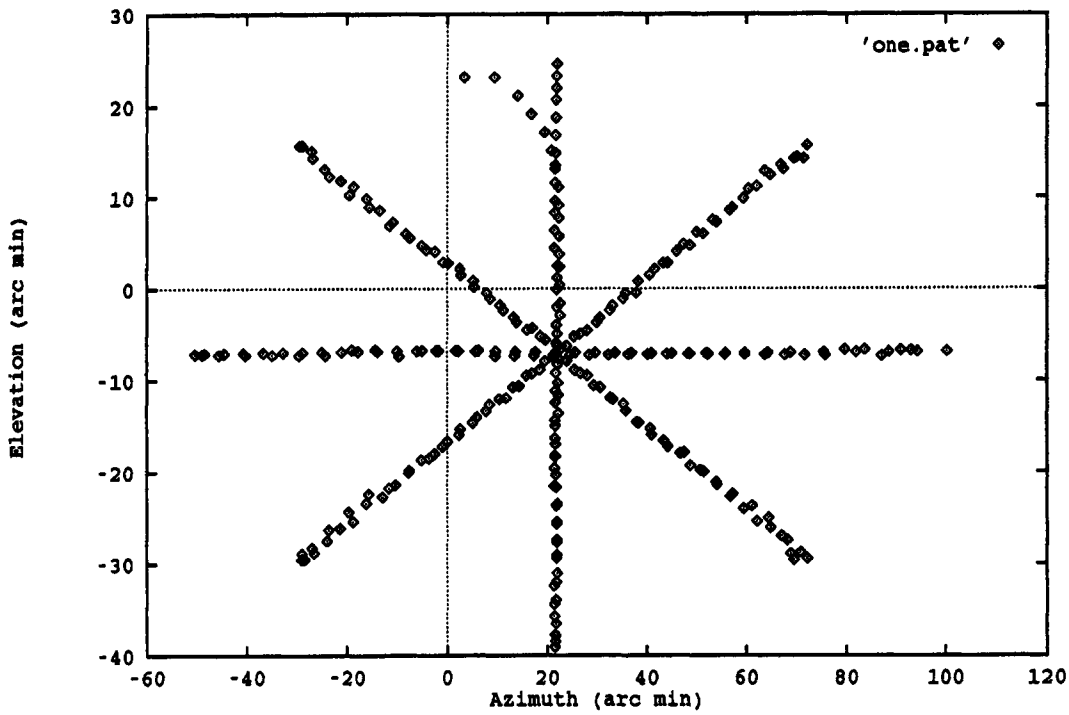


Figure 6: Plot of locations of observations of the brightness of radio source Cassiopeia A. The X axis is the azimuth offset from the calculated source position (arc minutes) and the Y axis is the elevation offset.

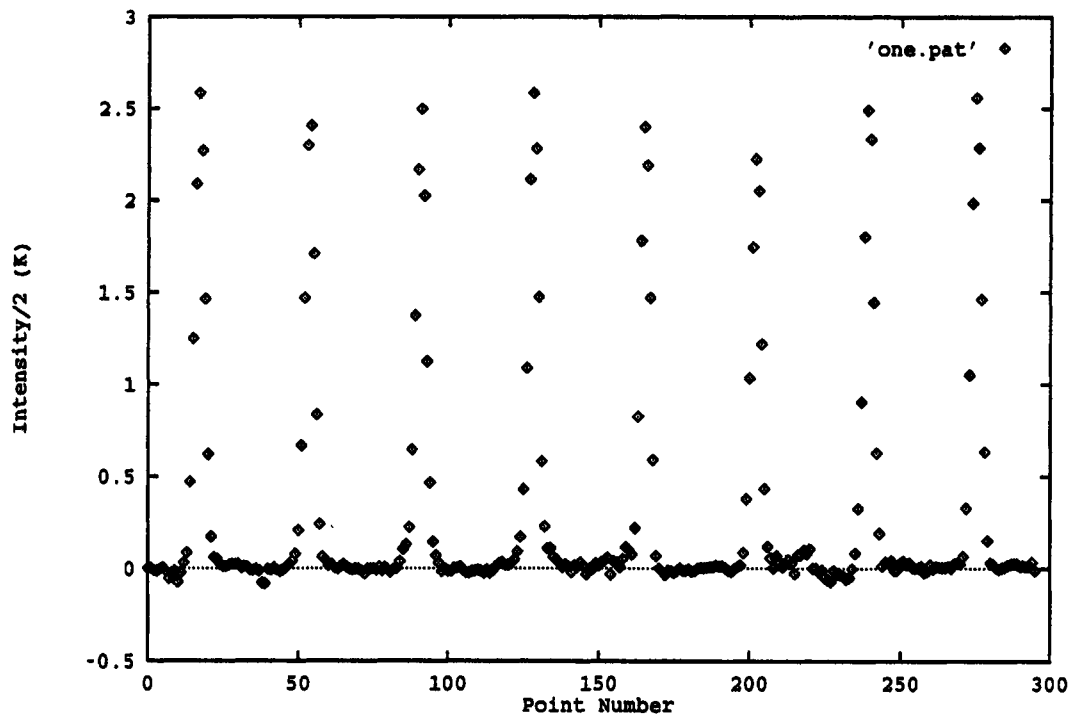


Figure 7: Plot of the half - intensity of the source as a function of point number. The X axis is data point number (total 296) and the Y axis is source intensity. The antenna passes over the source 8 times in these scans. The sky background has been subtracted from these data. (In this and all following plots, the signal levels were erroneously multiplied by a factor of 0.5, resulting in half-intensity plots)

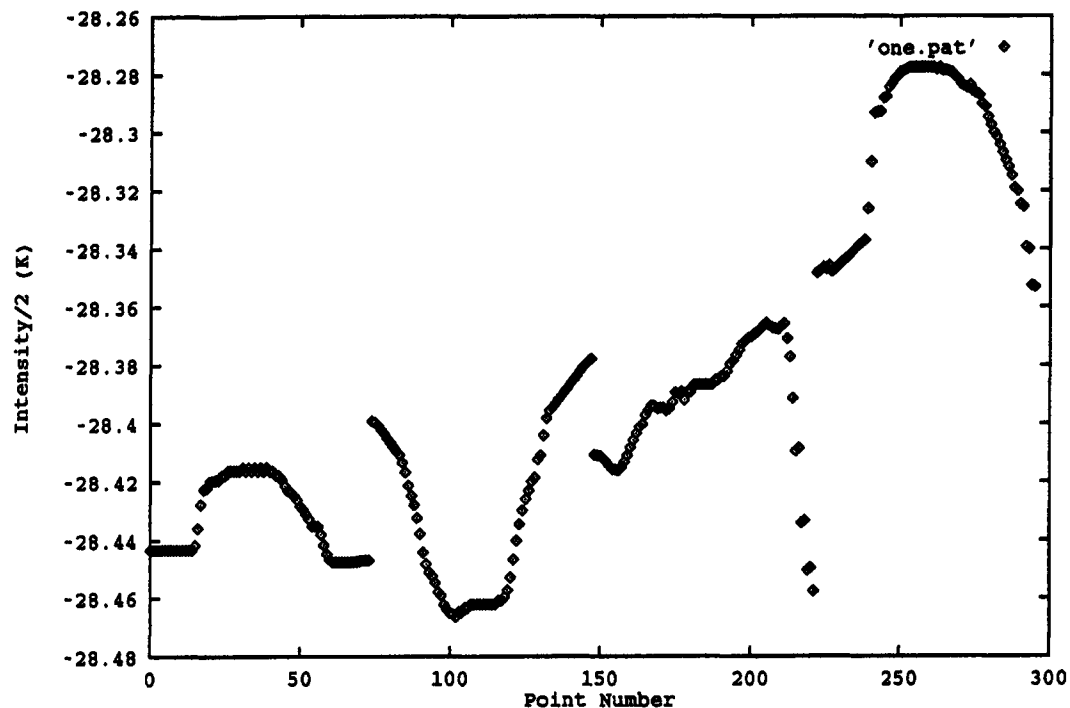


Figure 8: Plot of median filtered sky intensity estimate. These values are subtracted from the raw values before fitting. Notice that baselines changes of 10 % of the source brightness are being removed in the filtering process.

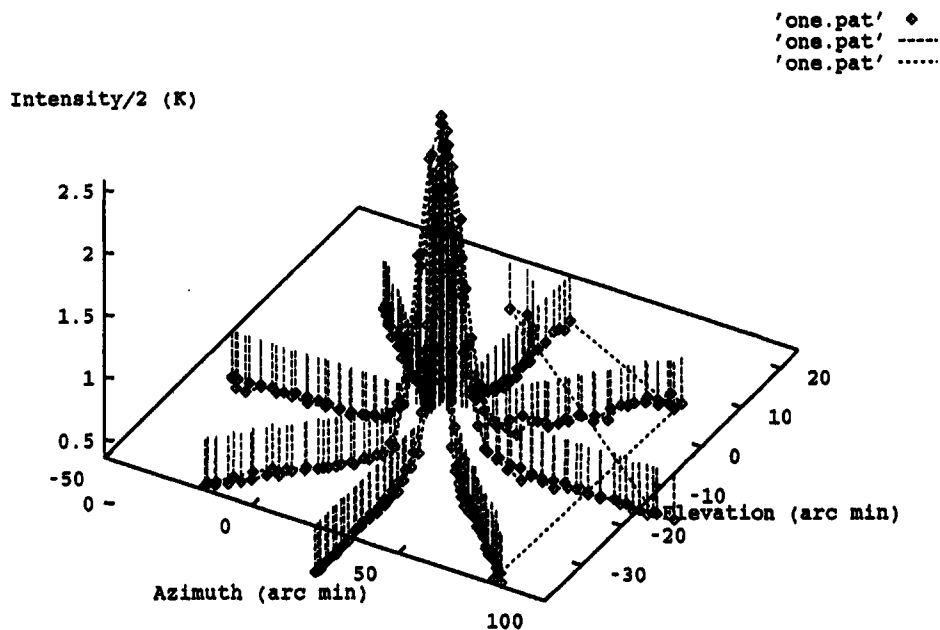


Figure 9: Plot of source intensity versus azimuth and elevation offsets.